OPTIONAL LABORATORY SESSIONS

- **Second-order NL Optics simulations**

Simulations using SNLO, a freeware software available for download at http://www.as-photonics.com/products/snlo

- **HHG simulations**

Simulations with a software developed at Politecnico di Milano, Italy.

- **Ultrashort Pulse Characterization**

This laboratory session is dedicated to the characterization of femtosecond pulses generated by mode-locked Er-doped fibre laser. This laser emits pulses centered at about 1560 nm at a repetition rate of 110 MHz. Second harmonic pulses at 780 nm will be generated in a periodically poled LiNBO3 crystal (PPLN). The fundamental and second harmonic spectra will be measured. A single shot autocorrelator will be aligned and calibrated for measuring the pulse duration of the second harmonic pulse. A GRENOUILLE measurement of the pulse amplitude and phase will also be made. Participants will receive more detailed laboratory notes.

- **Alignment of a hollow-core fiber for pulse compression**

Extreme ultraviolet (XUV) attosecond pulses are generated via the high order harmonic generation (HHG) process induced by focusing high peak intensity (1014 ÷ 1016 W/cm2) near infrared (NIR) pulses in a gas cell or in a gas jet.
For this kind of application Ti:Sapphire laser systems at the kHz repetition rate are usually employed to generate high energy (few mJ) NIR pulses with a time duration between 20 and 30 fs. In order to generate isolated attosecond pulses, these driving pulses have to be further compressed down to a few-femtoseconds.

The hollow-core fiber compressor is the most common and efficient device used to generate few-optical-cycle laser pulses with relatively high energy to drive attosecond pulse generation. The device is relatively simple and composed by a fused silica capillary filled with gas followed by a chirped mirror compressor. The laser light propagates in the fused silica capillary thanks to grazing incidence reflections at the inner surface of the dielectric. Furthermore, propagation losses ensure only the fundamental mode EH11 to propagate in a sufficiently long fiber. The input polarization is preserved during propagation in the fiber and the divergence of the beam at the output is very close to diffraction limit.

The hollow-core fiber is usually placed in a chamber filled with noble gases in order to achieve spectral broadening due to self-modulation in the medium. Self-modulation is a third order non-linear effect given by the refractive index (n) dependence on the intensity (I) of the propagating laser beam:

$$n = n_0 + n_2 I(r,t)$$

For a sufficiently high-intensity, in the spectrum of the laser pulse new frequencies appear along propagation in the non-linear medium. The instantaneous frequency is given by:

$$\omega_i(t) = -\frac{\partial \phi}{\partial t} \sim -\frac{n_2 \omega_0}{c} z \frac{\partial I(r,t)}{\partial t}$$

Where ϕ is the phase of the pulse. On the pulse rising edge red-shifted frequencies are generated, while frequencies towards the blue spectral region are generated on the trailing edge.
The gas medium needs to be properly chosen in order to have a sufficiently high ionization potential to ensure only purely third-order non-linear processes to occur. The fiber can be eventually operated in a pressure gradient configuration where the entrance of the capillary is kept under vacuum, thus preventing filamentation to occur before coupling into the fiber. The spectrally-broadened pulse obtained at the output of the capillary is then compressed to few-optical cycles by using a set of chirped mirrors, which allow to introduce negative dispersion and compensate for the residual positive chirp induced by propagation in the gas and through the fused silica window at the output of the fiber setup.

The best coupling is obtained by focusing the laser beam, at the fiber entrance, with a focal spot diameter equal to the 64% of the fiber core diameter, in this condition coupling efficiency can be more then 90%.

The aim of this training activity is to become familiar with the hollow-core fiber setup and its alignment, since it is a fundamental part of all the laser systems in attosecond laboratories.

The activity will consist in the following steps:

1) Mount and align a He-Ne laser
2) Estimate the size of the focus for optimal coupling into a 300-μm (core diameter) fiber
3) Mount and align a lens telescope for focusing the He-Ne beam
4) Mount the hollow-fiber capillary on a v-groove system with micrometric adjustments
5) Couple the laser into the hollow fiber by positioning the capillary in correspondence of the laser focus and aligning it with micrometric precision along the laser propagation direction
6) Extract the EH_{11} mode and measure the coupling efficiency

References

M. Nisoli et al, Appl. Phys. Lett. 68, 2793 (1996)
M. Nisoli et al, IEEE 4, 414 (1998)

• Thermal conductivity measurements by beam deflection spectroscopy

The thermal conductivities of different porous silicon samples [1,2] are determined by means of photothermal beam deflection spectroscopy (BDS) [3-7]. The experimental setup is schematically shown in figure 1. Light coming out from the excitation beam (EB) with an output wavelength of 532 nm and 200 mW output power (CST-H-532 nm-1000mW) is modulated electronically and heats the sample. Since the examined sample is opaque, it is assumed that the whole incident light energy is absorbed by its surface. Due to radiationless processes, the absorbed energy is converted into heat inducing temperature oscillations in the sample and fluid above it, which in turn causes a corresponding change in the index of refraction, and its gradients [4]. These variations are probed by a 632.8 nm output wavelength and 3 mW output power He–Ne laser (MELLES GRIOT, Model 9980TT) called the probe beam (PB). PB travels through the region of temperature oscillations, parallel to the surface of the sample (transverse BDS in its skimming configuration), and as a result of what it is deflected. The amplitude and phase of the PB deflection is determined by the use of position sensing detector (THORLABS, PDQ80 A). The amplitude and phase of the BDS signal are measured by a digital lock-in amplifier (SIGANAL RECOVERY 728 DSP LOCK-IN AMPLIFIER) connected to a PC for data storage and processing. The examined sample is placed on a 3D translation stage (THORLABS) to change its position in the *x*, *y*, and *z* directions and optimize the experimental configuration. The measurements are performed in air at room temperature. PB is focused by a 25 mm diameter lens of 10 mm focal distance (THORLABS) to have its waist of 50 μm radius over the sample, whereas EB is directed perpendicular to the surface of the sample by a broad band, flat mirror (400–750 nm, THORLABS) and shaped by a 25 mm diameter lens of 15 mm focal distance (THORLABS) to form a spot of around 1 mm diameter onto the sample's surface.

For each sample, the amplitude and phase of the BDS is measured as a function of the modulation frequency of EB. The thermal conductivity of the whole sample (porous layer and substrate), as well as of substrate without porous layer can be determined by comparing the measured results with theoretical values by the use of the least square fitting procedure [6]. To ensure high accuracy of the thermal conductivity determination, the measurements are conducted under 'thermally thick' conditions. This is achieved for thermal diffusion length of the temperature oscillations shorter than the thickness of the examined sample. Thus, the range of modulation frequency of the EB is chosen to be from 300 Hz to 3 kHz [7,8].

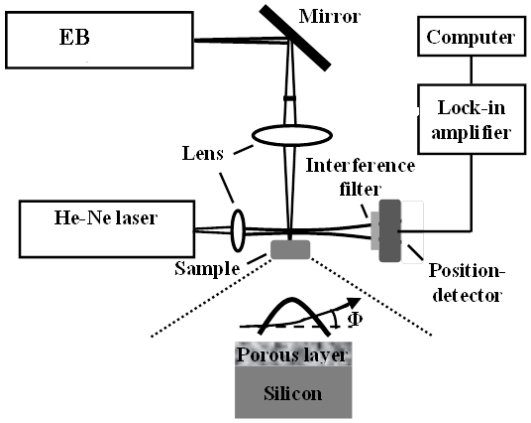

Figure 1. Experimental setup used for the BDS measurements. An excitation beam (EB) from continuous solid state laser, modulated electronically illuminates the surface of the sample. The induced periodic

variations in refractive index of air above the sample are sensed by the probe beam (PB) from a low power He-Ne laser and a position sensing detector connected to the lock-in amplifier and PC.

1. M. Pawlak, M. Chirtoc, N. Horny, J. Pelzl, J. Appl. Phys. **119**, 125108 – 125108 (2016).
2. M. Pawlak, A. Panas, A. Ludwig, A. D. Wieck, Thermochim. Acta **650**, 33 – 38, (2017).
3. D. Trefon-Radziejewska, J. Bodzenta, Opt. Mat. **45**, 2015, DOI: 10.1016/j.optmat.2015.03.007.
4. J. Bodzenta, A. Kazmierczak-Bałata, R. Bukowski, M. Nowak, B. Solecka, Int. J. Thermophys. **38(6)**, 93, (2017).
5. A. Kazmierczak-Bałata, J. Mazur, J. Bodzenta, D. Trefon-Radziejewska, L. Drewniak, Int. J. Thermophys. **35(12)**, 46, (2014).
6. D. Korte, M. Franko, Josa A. **32**, 61-74, (2015).
7. D. Korte, H. Cabrera, J. Toro, P. Grima, C. Leal, A. Villabona, M. Franko, Las. Phys. Lett., 2016, **13(12),** 1-12 (2016).
8. R.J. Martín-Palma, H. Cabrera, B. Martín-Adrados, D. Korte, E. Pérez-Cappe, Y. Mosqueda, M.A. Frutis, E. Danguillecourt, Mar. Res. Exp. **5**, 015004, (2018).